Article

Optically Transparent, Amphiphilic Networks Based on Blends of Perfluoropolyethers and Poly(ethylene glycol)

Zhaokang Hu, Liang Chen, Douglas E. Betts, Ashish Pandya, Marc A. Hillmyer, and Joseph M. DeSimone

J. Am. Chem. Soc., **2008**, 130 (43), 14244-14252 • DOI: 10.1021/ja803991n • Publication Date (Web): 04 October 2008

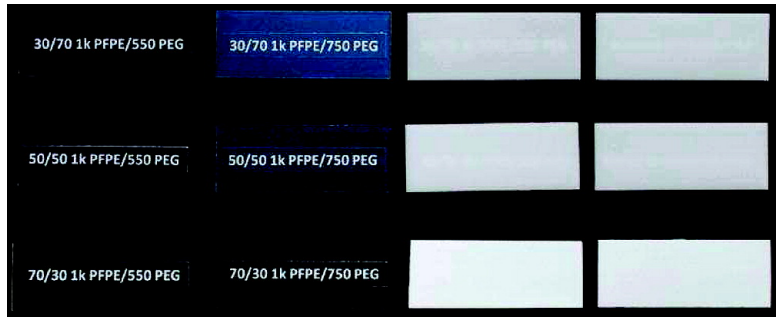

More About This Article

Additional resources and features associated with this article are available within the HTML version:

- Supporting Information
- Access to high resolution figures
- Links to articles and content related to this article
- Copyright permission to reproduce figures and/or text from this article

View the Full Text HTML

J|A|C|S
ARTICLES

Published on Web 10/04/2008

Optically Transparent, Amphiphilic Networks Based on Blends of Perfluoropolyethers and Poly(ethylene glycol)

Zhaokang Hu,[†] Liang Chen,[‡] Douglas E. Betts,[†] Ashish Pandya,[†] Marc A. Hillmyer,[‡] and Joseph M. DeSimone[†,§,*]

Department of Chemistry, University of North Carolina at Chapel Hill, Chapel Hill, North Carolina 27599, Department of Chemical Engineering, North Carolina State University, Raleigh, North Carolina 27695, and Department of Chemistry, University of Minnesota, Minneapolis, Minnesota 55455

Received June 5, 2008; E-mail: desimone@unc.edu

Abstract: Amphiphilic networks of perfluoropolyethers (PFPE) and poly(ethylene glycol) (PEG) have been achieved to yield optically transparent, mechanically robust films over a wide range of compositions. Telechelic diols of these oligomers were transformed to a photocurable dimethacryloxy form (DMA) and free radically cured at various composition weight ratios to yield free-standing films. Clear and colorless amphiphilic networks could be achieved when low molar mass versions of both the PFPE-DMA (1 kg/mol) and the PEG-DMA (550 g/mol) were used. The bulk morphologies of the samples were extensively characterized by a variety of techniques including ultraviolet−visible spectroscopy, differential scanning calorimetry, dynamic mechanic thermal analysis, small-angle X-ray scattering, atomic force microscopy, X-ray photoelectron spectroscopy, and optical microscopy, which strongly suggest that nanoscopic to macroscopic phase-separated materials could be achieved. By incorporating a threshold amount of PFPEs into PEG-based hydrogel networks, water swelling could be significantly reduced, which may offer a new strategy for a number of medical device applications. Along these lines, strong inhibition of nonspecific protein adsorption could be achieved with these amphiphilic network materials compared with an oligo(ethylene glycol)-based self-assembled monolayer coated surface.

Introduction

Amphiphilic networks have gained much attention and are the topic of several recent reviews.[1,2] In these systems, hydrophilic and hydrophobic phases are combined and then chemically cross-linked, thus generating an amphiphilic network. Such materials have been the target for developing novel applications such as contact lenses,[3,4] medical devices,[5,6] membranes,[7,8] enzyme catalysts,[9,10] and drug delivery.[11−13] Most amphiphilic networks extensively studied consist of a hydrophilic and a hydrophobic phase. As a unique class of materials, fluoropolymers possess a combination of properties, including high thermal and chemical stability, low surface energy, and low flammability. In addition, fluoropolymers exist in forms ranging from thermoplastics to elastomers. They have found many applications in building, automotive, and petrochemical industries, microelectronics, aerospace, and optics.[14] However, because of the immiscibility between fluorophilic and hydrophilic or hydrophobic segments, limited amphiphilic networks comprising fluorophilic chain segments have been reported.

Bruns and Tiller reported a class of nanophasic hydrophilic/fluorophilic networks that were achieved by photochemically curing blends of a dimethacryloxy-form perfluoropolyether (PFPE) with perfluorosilyl-protected poly(hydroxy ethylacrylate) (PHEA).[15] This is not a straightforward method to form amphiphilic networks as it requires the perfluorosilyl protecting groups on the PHEA chain segments to be cleaved in a subsequent procedure involving soaking the cured films in hydrochloric acid and tetrahydrofuran for 24 h. The acid-deprotection step is thought to deleteriously affect the fluorinated nature of the surfaces of the network materials. Wooley et al. recently reported the formation of amphiphilic networks derived from the cross-linking of poly(ethylene glycol) with hyper-

[†] University of North Carolina at Chapel Hill.
[‡] University of Minnesota.
[§] North Carolina State University.

(1) Erdodi, G.; Kennedy, J. P. *Prog. Polym. Sci.* **2006**, *31*, 1.
(2) Patrickios, C. S.; Georgiou, T. K. *Curr. Opin. Colloid Interface Sci.* **2003**, *8*, 76.
(3) Nicolson, P. C.; Vogt, J. *Biomaterials* **2001**, *22*, 3273.
(4) Friends, G. D.; Kunzler, J. F.; Ozark, R. M. *Macromol. Symp.* **1995**, *98*, 619.
(5) Shamlou, S.; Kennedy, J. P.; Levy, R. P. *J. Biomed. Mater. Res.* **1997**, *35*, 157.
(6) Kennedy, J. P.; Rosenthal, K. S.; Kashibhatla, B. *Des. Monomers Polym.* **2004**, *7*, 485.
(7) Du Prez, F. E.; Goethals, E. J.; Schue, R.; Qariouh, H.; Schue, F. *Polym. Int.* **1998**, *46*, 117.
(8) Isayeva, I. S.; Gent, A. N.; Kennedy, J. P. *Polym. Prepr. (Am. Chem. Soc., Div. Polym. Chem.)* **2002**, *43*, 616.
(9) Bruns, N.; Tiller, J. C. *Nano Lett.* **2005**, *5*, 45.
(10) Savin, G.; Bruns, N.; Thomann, Y.; Tiller, J. C. *Macromolecules* **2005**, *38*, 7536.
(11) Chen, D.; Kennedy, J. P.; Kory, M. M.; Ely, D. L. *J. Biomed. Mater. Res.* **1989**, *23*, 1327.
(12) Keszler, B.; Kennedy, J. P.; Mackey, P. W. *J. Controlled Release* **1993**, *25*, 115.
(13) Brown, G. O.; Bergquist, C.; Ferm, P.; Wooley, K. L. *J. Am. Chem. Soc.* **2005**, *127*, 11238.
(14) Ameduri, B.; Boutevin, B. *J. Fluorine Chem.* **2005**, *126*, 221.
(15) Bruns, N.; Tiller, J. C. *Macromolecules* **2006**, *39*, 4386.

10.1021/ja803991n CCC: $40.75

branched perfluorobenzyl ether.[16,17] The unusual topology, morphology, surface, and mechanical properties have been systematically studied.[18,19] Although these materials show interesting antifouling properties,[20] they appear to be heterogeneous because of a wide degree of incompatibility along the architectural and compositional axes.[21]

Thus far in the literature, the existence of a fluorophilic/hydrophilic amphiphilic network possessing good miscibility between the two components in a wide composition ratio has not been reported. Herein for the first time, we report the surprising observation that the low molar mass dimethacryloxy-terminated PFPE (1 kg/mol) and dimethacryloxy-terminated PEG (550 g/mol) form optically transparent liquid blends in all composition ratios. When the higher molar mass PFPE (4 kg/mol) was mixed with PEGs (550 and 750 g/mol), a series of milky-white emulsions formed. All liquid blends with reactive forms of these oligomers could then be photochemically cured to form optically transparent to opaque materials in one step.

Experimental Section

Materials. 1,1,1,3,3-Pentafluorobutane (Solkane 365 MFC) was purchased from Micro-Care. The 1 and 4 kg/mol PFPE diols (Fluorolink D10 and Fomblin ZDOL 4000) were purchased from Solvay Solexis. Tetrabutyltin diacetate (DBTDA), α-hydroxycyclohexyl phenylketone (HCPK), 2-isocyanatoethyl methacrylate (IEM), poly(ethylene glycol) dimethacrylates (PEG-DMA, 550 and 750 g/mol), hexa(ethylene glycol)mono-11-mercaptoundecyl ether, canine plasma fibrinogen, bovine serum albumin (BSA), and all solvents used were purchased from Sigma-Aldrich. HyClone phosphate-buffered saline (PBS, 1X, 0.0067 M PO_4, without calcium, without magnesium, 0.1 μm sterile filtered) was purchased from Fisher. Cell culture plates (48 well, flat bottom) used for protein adsorption research were purchased from Corning, Inc.

Synthesis of PFPE-DMAs. PFPE-DMAs were synthesized as previously reported.[22] Briefly, PFPE diol (1 or 4 kg/mol) was first dissolved in 1,1,1,3,3-pentafluorobutane and reacted with a 2.05:1 molar ratio of IEM at 45 °C for 24 h, using 0.1 wt % DBTDA as a catalyst. The solution was then passed through a chromatographic column filled with alumina (2 × 10 cm). After the solvent was evaporated, the product was filtered through a 0.2-μm poly(ether sulfone) filter to yield a clear, colorless, viscous oil.

Photocuring of PFPE/PEG Amphiphilic Networks. Commercial PEG-DMA with molar masses of 550 or 750 g/mol was first passed through a chromatographic column (alumina, 2 × 10 cm) to remove any inhibitor. Purified 550 g/mol PEG-DMA was then added into the desired amount of the 1 kg/mol PFPE-DMA precursor (composition weight ratios of 30/70, 50/50, and 70/30 were studied) to form a mixture, followed by the addition of 0.2 wt % of HCPK photo initiator. A colorless and clear, homogeneous liquid blend of 1k/mol PFPE-DMA and 550 g/mol PEG-DMA was obtained after vortexing (Vortex Genie 2, Scientific Industries, Inc.) the mixture for approximately 5 min at room temperature to dissolve the photo initiator. To achieve a fully cured PFPE/PEG network, the homogeneous PFPE/PEG liquid blend was simply cast onto a clean silicon wafer followed by subsequent UV irradiation (Electronlite UV curing chamber model no. 81432-ELC-500, $\lambda = 365$ nm) for 10 min under N_2 purge. This resulted in a completely clear, elastomeric material. Opaque 4k PFPE/PEG blends could be achieved following a similar protocol by blending the higher molar mass 4 kg/mol PFPE-DMA with either the 550 or 750 g/mol PEG-DMA.

Ultraviolet−Visible Spectroscopy. UV−vis transparency was performed with a Shimadzu UV-3600 UV−vis NIR spectrophotometer over the wavelength range of 200−800 nm. Thin films of ca. 1 mm were measured for optical transparency with the percent transmittance at 550 nm (the solar maximum) reported.

Dynamic Mechanical Thermal Analysis. DMTA measurements were performed in a 210 Seiko Dynamic mechanical spectrometer, operated at a fixed frequency (1 Hz) in tension mode. The temperature was varied from −150 to 150 °C with a heating rate of 2 °C/min.

Differential Scanning Calorimetry. DSC curves were recorded with a Seiko DSC 120 in the temperature range from −150 to 100 °C, at a scanning rate of 10 °C/min.

Atomic Force Microscopy. Cross sections were imaged using a Multimode atomic force microscope in tapping mode from Veeco Metrology group equipped with Nanoscope III control station and silicon cantilevers from Mikromasch USA with resonance frequencies of about 160 kHz, spring constants of 5.0 N/m, and radii of less than 10 nm.

Optical Microscopy. Ultrathin sections cut by microtome were studied at 40× magnification under unpolarized light using an optical microscope (Olympus BH2) equipped with a SpotRT camera and photographic system.

Small-Angle X-ray Scattering. SAXSess instrument (Anton Paar) at the University of Minnesota was utilized to probe the microstructure in the cross-linked PFPE/PEG blends. The cross-linked film was placed in a Cu sample holder, and scattering was measured at room temperature for 5 min, operating at 40 kV and 50 mA. Scattering signal was not corrected for instrumental broadening caused by the line-collimated incident beam, and then integrated into a 1D plot of intensity versus the scattering vector q. Finally, scattering intensity was normalized with respect to the incident beam intensity.

Mechanical Properties. Stress−strain measurements were performed for rectangular samples (1 × 10 × 20 mm^3) at ambient temperature on an Instron model 5566 system using a 10 kN load cell at a crosshead speed of 5 mm/min. An extensometer of 15-mm gauge length was used to measure the strain accurately. The Young's modulus was determined from the stress−strain curves. Four replicates were performed for each sample.

Swelling Experiments. Swelling measurements were performed by soaking fully cured PFPE/PEG films in deionized water for 24, 48, and 72 h. The weight percent swelling ratio was determined using the following equation: wt % swelling = 100% * (W_{wet} − W_{dry})/W_{dry}. For accurate evaluation of the weight of the dried film, the original film was dried to a constant weight in a vacuum oven at 100 °C for 24 h. The weight of the water-swelled film was recorded after quickly blotting the film between two sheets of filter paper. No difference was visually observed for all PFPE/PEG films during the soaking treatment.

Static Contact Angle Measurement. Static contact angles were measured using a KSV Instruments LCD CAM 200 optical contact angle meter at room temperature (23 °C). All measurements were carried out with drops that had a total volume of 10 μL on the surface of each fully cured film using a 1000-μL screw-top syringe.

X-ray Photoelectron Spectroscopy. XPS analysis was performed using a Kratos Axis Ultra equipped with a monochromated Al Kα X-ray source. Photoelectrons at pass energies ranging from 20 to 80 eV were collected with a concentric hemispherical analyzer and detected with a delay line detector. All data were collected at 90° from the surface normal takeoff angle and processed with Kratos Vision software (version 2.2.6). The binding energy component in

(16) Gan, D.; Mueller, A.; Wooley, K. L. *J. Polym. Sci., Part A: Polym. Chem.* **2003**, *41*, 3531.
(17) Gudipati, C. S.; Greenlief, C. M.; Johnson, J. A.; Prayongpan, P.; Wooley, K. L. *J. Polym. Sci., Part A: Polym. Chem.* **2004**, *42*, 6193.
(18) Xu, J.; Bohnsack, D. A.; Mackay, M. E.; Wooley, K. L. *J. Am. Chem. Soc.* **2007**, *129*, 506.
(19) Brown, G. O.; Bergquist, C.; Ferm, P.; Wooley, K. L. *J. Am. Chem. Soc.* **2005**, *127*, 11238.
(20) Gudipati, C. S.; Finlay, J. A.; Callow, J. A.; Callow, M. E.; Wooley, K. L. *Langmuir* **2005**, *21*, 3044.
(21) Bartels, J. W.; Cheng, C.; Powell, K. T.; Xu, J.; Wooley, K. L. *Macromol. Chem. Phys.* **2007**, *208*, 1676.
(22) Rolland, J. P.; Van Dam, R. M.; Schorzman, D. A.; Quake, S. R.; DeSimone, J. M. *J. Am. Chem. Soc.* **2004**, *126*, 2322.

Scheme 1. Synthetic Scheme of PFPE/PEG Networks via a Precursor Approach

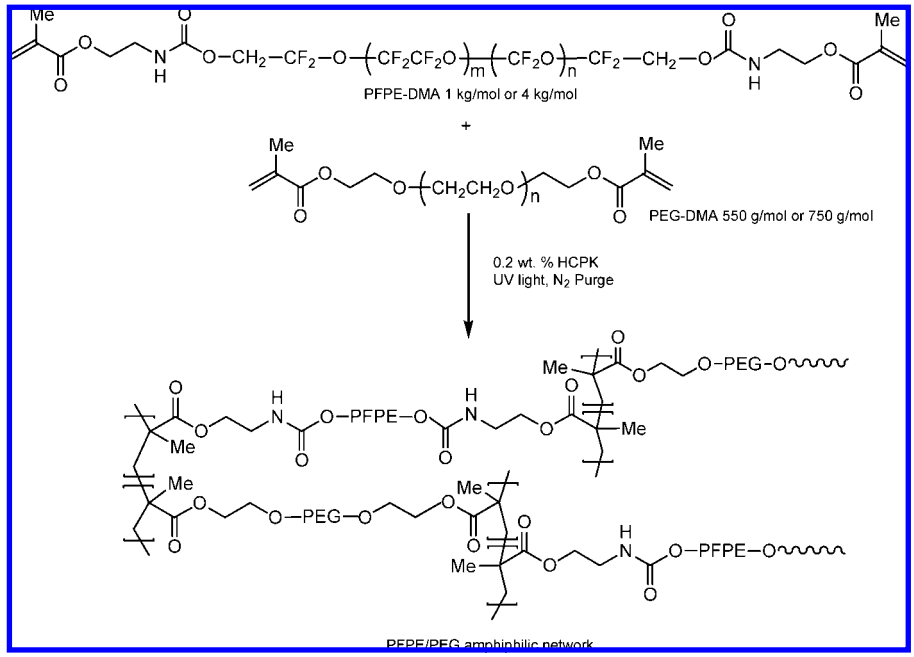

the C_{1s} region (CF_2CF_2O) was referred to 293.5 eV, and all other element scans were shifted accordingly.

Surface Preparation for Protein Adsorption. A Fisher brand standard glass slide (3″ × 3″) was first cut into 5 × 5 mm^2 pieces and boiled in piranha solution ($H_2SO_4/H_2O_2 \approx 3:1$) at 90 °C for 30 min, followed by thorough washing in deionized water and ethanol, and dried with a stream of N_2. Oligo(ethylene glycol) (OEG) self-assembled monolayers (SAMs) on gold surfaces containing hexa-(ethylene glycol)mono-11-mercaptoundecyl ether ($HS\text{-}C_{11}\text{-}EG_6$) were prepared from a 1 mM solution of $HS\text{-}C_{11}\text{-}EG_6$ thiol dissolved in degassed, absolute ethanol by placing gold substrates in the solution for 24 h at room temperature.[23] To accurately evaluate protein adsorption, untreated pieces of 5 × 5 mm^2 gold foil (0.1 mm, Sigma-Aldrich) were used as a negative control. All studied surfaces were rinsed with deionized water and ethanol before the protein solution was applied.

Protein Adsorption. An enzyme-linked immunosorbent assay (ELISA) was used to measure fibrinogen adsorption on the surfaces of cured PFPE/PEG amphiphilic networks.[24] The 5 × 5 mm^2 thin films were put onto a 48-well plate and incubated in 500 μL of 1 mg/mL fibrinogen in PBS at 37 °C for 90 min. The films were then removed from the protein solution with forceps, rinsed five times with PBS solution (pH 7.4), and incubated in a new 48-well plate with 500 μL of 1 mg/mL BSA in PBS at 37 °C for 90 min to block the areas unoccupied by fibrinogen. The films were taken out again, washed five times with PBS, and moved to another 48-well plate, followed by the addition of 500 μL of horseradish peroxidase (HRP) conjugated antifibrinogen (Antogen Bioclear, working dilution of 1:10 000) into each well and incubated at 37 °C for 30 min. After being washed five times with PBS, the samples were transferred to another clean 48-well plate and incubated in 500 μL of TMB substrate (containing HRP, Pierce) at 37 °C for 20 min. The enzyme-induced color reaction was stopped by adding 500 μL of 1 M H_2SO_4 solution. The solution then changed color from light blue to light yellow. Finally, the absorbance of the light intensity was determined at 450 nm by a microplate reader (SpectraMax M5, Molecular Devices).

(23) Troughton, E. B.; Bain, C. D.; Whitesides, G. M.; Nuzzo, R. G.; Allara, D. L.; Porter, M. D. *Langmuir* **1988**, *4*, 365.
(24) Zhang, Z.; Chao, T.; Chen, S.; Jiang, S. *Langmuir* **2006**, *22*, 10072.

Results and Discussion

To our surprise, the low molar mass 1 kg/mol PFPE-DMA was completely miscible with the low molar mass 550 g/mol PEG-DMA at ambient temperature. Clear liquid blends of these two prepolymers were obtained in all composition weight ratios after vortexing the mixtures for 5 min. Completely clear liquid blends could be formed in the composition weight ratio of 70/30 1k PFPE/750 PEG or higher when mixing the 1 kg/mol PFPE-DMA with the 750 g/mol PEG-DMA. The liquid blend was slightly hazy when the composition weight ratio was decreased to 50/50 1k PFPE/750 PEG and became hazier when further decreased to 30/70 1k PFPE/750 PEG in this case. However, kinetically stable, milky-white emulsions formed when adding the higher molar mass 4 kg/mol PFPE-DMA into PEG-DMAs (both 550 and 750 g/mol) in the composition weight ratio of 70/30 PFPE/PEG or higher. Less stable opaque liquid blends were yielded in lower composition ratios that separated in hours. Further studies indicated that the methacryloxy end group is not necessary to form these clear liquid blends. A clear liquid blend was also achieved by mixing the 1 kg/mol PFPE diol with either the 550 g/mol PEG-DMA or the 600 g/mol PEG diol while a milky-white emulsion was formed by mixing the 1 kg/mol PFPE-DMA with the 600 g/mol PEG diol.

These liquid blends were easily cured free radically to yield free-standing films in one step (Scheme 1). Typically, the liquid blends were first vortexed at ambient temperature for 5 min to dissolve the photoinitiator (0.2 wt % of HCPK). They were then cast onto a clean flat silicon wafer followed by subsequent UV irradiation for 10 min under N_2 purge. The resulting series of amphiphilic PFPE/PEG films varied from optically transparent to opaque, dependent upon the molar masses and composition ratios as shown in Figure 1. In each series (i.e., 1 or 4 kg/mol PFPE-DMA with 550 or 750 g/mol PEG-DMA), blends in three composition weight ratios (30/70, 50/50, and 70/30) were fabricated for further study. The optical transparency of the resulting films was quantitatively elucidated by measuring the transmittance at 550 nm. As seen in Table 1, all transparent films showed a high transmittance of ca. 98% in the range of

Figure 1. Photograph of fully cured PFPE/PEG blend films both optically transparent and opaque formed with different composition ratios and molar masses. A label is underneath each sample. Onto this label is typed descriptive text, only readable for the optically transparent and hazy samples.

400−800 nm. For 1k PFPE/750 blends, as the composition ratio was decreased from 70/30 to 30/70, the film gradually turned hazy with the transmittance decreasing from ca. 98.1 to 83.7%. With macrophase separation for the 4k PFPE/PEG blends, most of the visible light cannot go through the samples, resulting in a transmittance of less than 40%. The transmittance further decreased to 11.6% for the 70/30 4k PFPE/550 PEG blend and 8.0% for the 70/30 4k PFPE/750 PEG blend, because of more visible light being scattered inside the samples.

The morphologies of the fully cured PFPE/PEG films were studied by DMTA and are shown in Figure 2. Two transitions were found for the cured 1 kg/mol PFPE-DMA, the glass transition (T_g) at 54.5 °C was assigned to the methacrylic cross-linking end groups of the PFPE domains, and a secondary relaxation at −80.4 °C was assigned to the PFPE domains of the main chains located away from cross-links.[25] For the blends of the 1 kg/mol PFPE-DMA with the 550 g/mol PEG-DMA, the methacrylic cross-linking groups of the PFPE segments were miscible with the PEG domains and formed a mixed phase after cross-linking, corresponding to the broad T_g at 10−50 °C as shown in Figure 2a, which shifted to a higher temperature upon increasing the PFPE in the composition ratio. The secondary relaxation for PFPE domains located away from the cross-links was severely restricted by cross-linking from the mixed PFPE/PEG phase. In this case, the β-transition could not be detected by either DMTA or DSC (Figures 2a and 3a). However, the broad T_g for the blends indicates a level of microheterogeneity that is reflected in nanoscale phase separation.

When a higher molar mass 750 g/mol PEG-DMA was blended with the 1 kg/mol PFPE-DMA, the methacrylic cross-linking end groups of the PFPE segments appeared to be compatible with PEG domains, while the secondary relaxation of the PFPE domains located away from the cross-links was not perturbed to any significant extent by the miscible methacrylic cross-linked PEG-rich domains. The short-range molecular motions within PFPE domains became enhanced, and the β-transition appeared to be visible in DSC (still invisible in DMTA), which cannot be clearly detected for the 1k PFPE/550 PEG blends in a similar condition (Figure 3a). As the cross-link density was decreased by incorporating more 750 g/mol PEG-DMA into the blend networks, the effect of the restrictions from the methacrylic cross-linked phase to the secondary relaxation of PFPE domains away from the cross-links became weaker and weaker, to the point that in the composition ratio of 50/50 1k PFPE/750 PEG, the mixture became immiscible and the blend appeared to be hazy. As a result, the broad T_g for the mixed phase shifted from 50 to −35 °C. Unlike the 1 kg/mol PFPE-DMA, a lower T_g around −130 °C for the dominant PFPE phase located far away from the cross-links was observed with a broad T_g of the minor phase located in the vicinity of the cross-links around 30 °C for the 4 kg/mol PFPE-DMA. The highly fluorophilic 4 kg/mol PFPE-DMA was immiscible with the PEG-DMAs. It resulted in a series of optically opaque blends with PEG-DMAs of various molecular weights in all composition ratios. Two T_g's were clearly detected by both DMTA and DSC for the 4 kg/mol PFPE-DMA blends, as shown in Figures 2c,d and 3b. As the content of the 4 kg/mol PFPE-DMA was increased in these blends, the secondary relaxation within PFPE domains became more pronounced with a more enhanced peak for the β-transitions observed at −130 °C.

The bulk morphologies of 1 kg/mol PFPE/PEG blends were investigated by AFM phase images on the cross sections of cryo-fractures. The AFM results are consistent with the observations by DMTA. Nanophase separation was observed even for the blends with a single T_g. This is not unexpected based on the DMTA data, which indicate some nanophase separation in the cured 1 kg/mol PFPE-DMA homopolymer. As shown in Figure 4a, uniform nanophase separation occurred with a domain size of 19.7 ± 3.2 nm for the cured 30/70 1k PFPE/550 PEG sample. These domains were completely separated by continuous walls as thin as 5 nm, which are believed to be rich in the stiffer PFPE phase. As the composition ratio was increased to 50/50 1k PFPE/550 PEG (Figure 4b), most of the domains remained well separated with an average domain size of 21.4 ± 5.0 nm while some of them aggregated in certain locations and smaller 10-nm domains were found between the larger domains. As the composition ratio was further increased to 70/30 1k PFPE/550 PEG (Figure 4c), the cross section became less heterogeneous, making the domain size immeasurable.

The 1k PFPE/550 PEG blends and associated cross-linked homopolymers were also analyzed by small-angle X-ray scattering (SAXS) in Figure 5. The cross-linked 1 kg/mol PFPE-DMA sample exhibited a peak in the scattered intensity at about 2 nm^{-1} corresponding to a domain spacing of about 3 nm. This is likely due to clustering of the polymerized methacrylate end groups in the highly fluorinated matrix, thus leading to compositional heterogeneity at length scales comparable to the PFPE chain dimensions. A similar peak was not observed for the cross-linked 550 g/mol PEG-DMA sample. In the PEG-DMA case, it may be that the scattering contrast or level of incompatibility is not high enough to observe a well-resolved peak. The scattering data from the three 1k PFPE/550 PEG blends exhibited two similar features: (i) enhanced scattering at low q and (ii) a peak or a broad shoulder at about 1 $nm^{-1} < q < 2$ nm^{-1} (ca. 3−6 nm length scale). We posit that the peak (shoulder) is again associated with scattering from domains of the polymerized (now copolymerized) methacrylate groups in a matrix consisting of a mixture of PEG and PFPE. However, the increased scattering intensity at $0.1 < q < 1$ (ca. 6−60-nm length scales) suggests compositional heterogeneities over a range of larger length scales, consistent with the AFM images shown in Figure 4. Both the scattering intensity at low q and the length scale associated with the peak (shoulder) increase with increasing PEG content. This suggests that the domain sizes on average are increasing with increasing PEG content in these blends.

For the 1k PFPE/750 PEG blends, the samples at first appeared milky when a small amount of the 1 kg/mol PFPE-

(25) Priola, A.; Bongiovanni, R.; Malucelli, G.; Pollicino, A.; Tonelli, C.; Simeone, G. *Macromol. Chem. Phys.* **1997**, *198*, 1893.

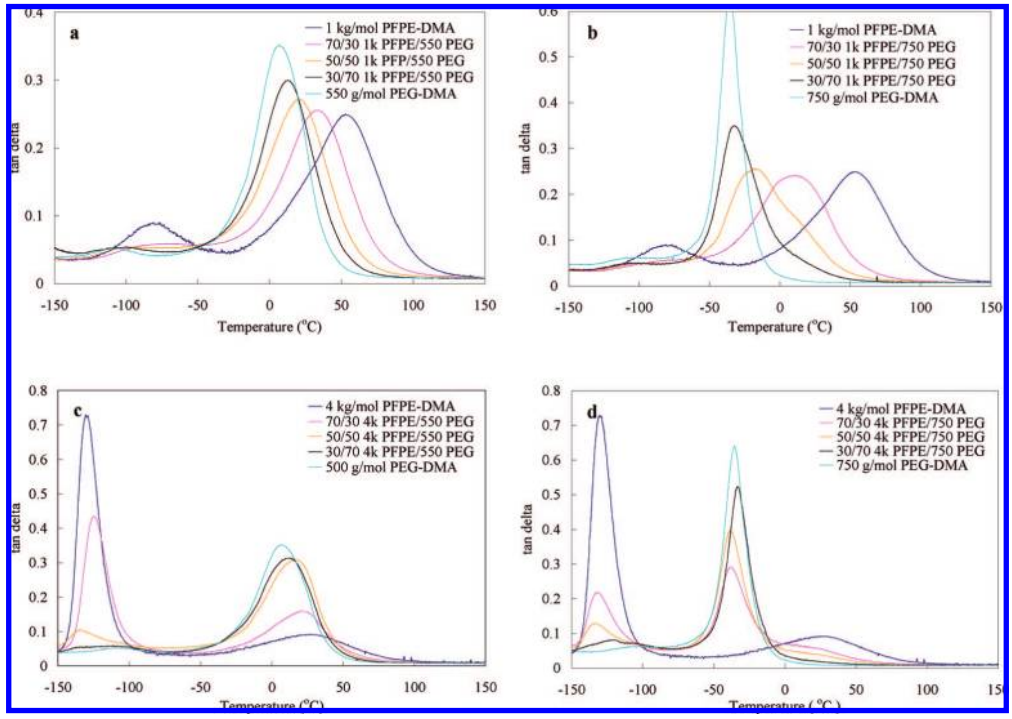

Figure 2. DMTA spectra of the fully cured PFPE/PEG amphiphilic networks of varying component ratios and molar masses. (a) 1k PFPE/550 PEG, (b) 1k PFPE/550 PEG, (c) 4k PFPE/550 PEG, and (d) 4k PFPE/750 PEG.

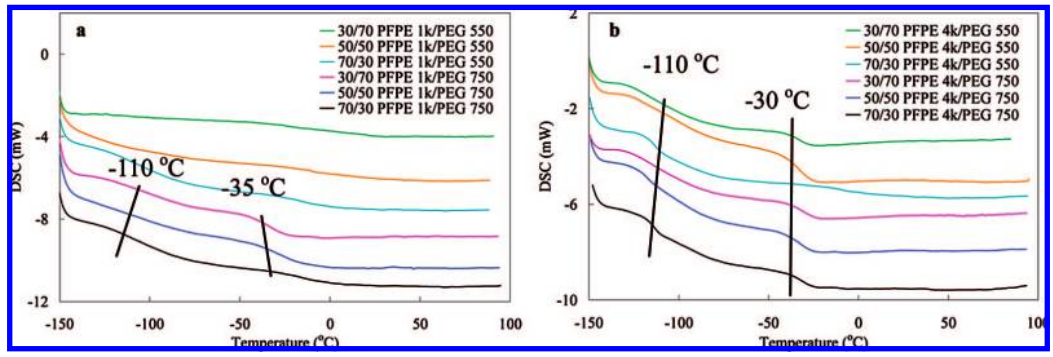

Figure 3. DSC spectra of the fully cured PFPE/PEG blends. (a) PFPE 1k/PEG series and (b) PFPE 4k/PEG series.

Table 1. Summary of Characterization Data for All PFPE/PEG Blends

PFPE-DMA mol wt (kg/mol)	PEG-DMA mol wt (g/mol)	PFPE/PEG wt ratio	transmit at 550 nm	Young's modulus (MPa)	swelling ratio in water (wt %)			static contact angle (deg)	
					24 h	48 h	72 h	air interface	sub interface
1	n/a	n/a	n/a	89.9 ± 10.4	0.6 ± 0.1	0.5 ± 0.2	0.4 ± 0.1	110.2 ± 2.0	100.0 ± 2.1
1	550	70:30	98.6 ± 0.2	66.9 ± 4.2	2.4 ± 0.2	2.8 ± 0.1	2.9 ± 0.1	106.7 ± 1.3	74.7 ± 1.4
1	550	50:50	98.0 ± 0.1	53.3 ± 2.7	7.3 ± 0.1	8.0 ± 0.2	7.6 ± 0.2	109.8 ± 0.4	63.0 ± 1.3
1	550	30:70	98.7 ± 0.1	48.6 ± 2.2	14.0 ± 0.4	13.9 ± 0.7	14.6 ± 0.6	109.1 ± 1.6	58.3 ± 1.8
n/a	550	n/a	n/a	40.3 ± 2.4	26.9 ± 0.4	27.6 ± 0.2	27.3 ± 0.5	70.3 ± 2.3	52.8 ± 2.0
1	750	70:30	98.1 ± 0.1	28.1 ± 0.9	4.7 ± 0.1	5.0 ± 0.5	4.9 ± 0.5	112.3 ± 2.8	69.3 ± 2.3
1	750	50:50	92.4 ± 0.1	22.5 ± 1.4	14.9 ± 0.4	15.2 ± 0.4	14.9 ± 0.2	108.1 ± 2.0	65.3 ± 3.4
1	750	30:70	83.7 ± 0.1	19.8 ± 0.4	25.1 ± 0.2	25.4 ± 0.3	24.9 ± 0.2	108.0 ± 1.2	56.6 ± 1.1
n/a	750	n/a	n/a	16.5 ± 0.7	51.4 ± 0.4	49.3 ± 2.9	50.8 ± 0.9	72.8 ± 1.6	56.2 ± 1.7
4	550	70:30	11.6 ± 0.2	16.9 ± 0.5	4.0 ± 0.2	4.3 ± 0.1	5.5 ± 0.4	128.6 ± 3.8	71.4 ± 2.9
4	550	50:50	36.0 ± 0.2	23.4 ± 1.1	10.0 ± 0.2	10.1 ± 0.2	11.0 ± 1.8	113.8 ± 1.0	63.0 ± 2.5
4	550	30:70	38.5 ± 0.3	30.2 ± 1.5	14.0 ± 0.4	13.9 ± 0.7	14.6 ± 0.6	108.0 ± 2.9	64.3 ± 3.1
4	750	70:30	8.1 ± 0.1	10.5 ± 0.9	9.8 ± 0.1	13.0 ± 0.5	12.9 ± 0.9	132.7 ± 4.3	65.2 ± 3.5
4	750	50:50	35.2 ± 0.1	13.1 ± 0.7	22.6 ± 0.3	21.2 ± 0.4	21.1 ± 0.2	127.7 ± 2.2	64.8 ± 4.5
4	750	30:70	41.6 ± 0.2	14.8 ± 1.6	31.1 ± 0.1	30.7 ± 0.8	30.0 ± 0.2	112.0 ± 2.2	65.3 ± 2.1
4	n/a	n/a	n/a	7.0 ± 0.3	0.2 ± 0.1	0.1 ± 0.1	0.1 ± 0.1	108.0 ± 1.3	99.1 ± 1.8

DMA was incorporated, but as the content of PFPE-DMA was increased, the blends became optically transparent. This phenomenon can be explained by the AFM phase images shown in Figure 4. In Figure 4d, a cocontinuous morphology was

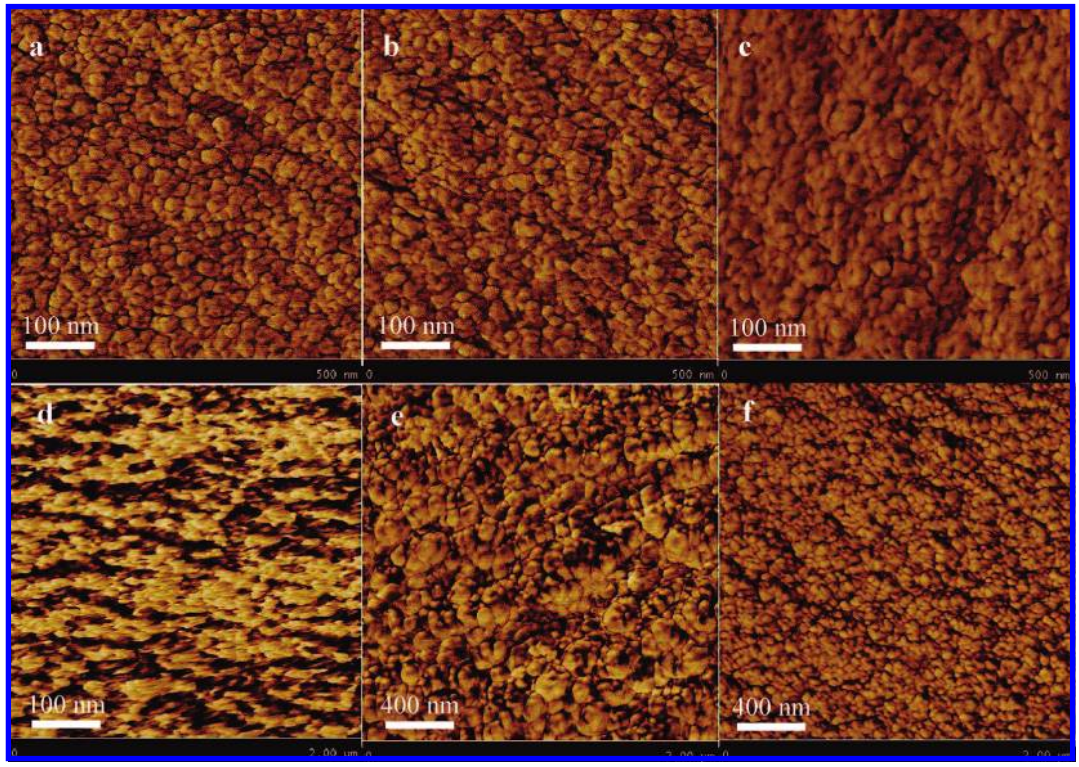

Figure 4. AFM phase mode images on cross sections of (a) 30/70 1k PFPE/550 PEG, (b) 50/50 1k PFPE /550 PEG, (c) 70/30 1k PFPE/550 PEG, (d) 30/70 1k PFPE/750 PEG, (e) 50/50 1k PFPE/750 PEG, and (f) 70/30 1k PFPE/750 PEG. In the hard tapping mode, PFPE shows dark and PEG show light.

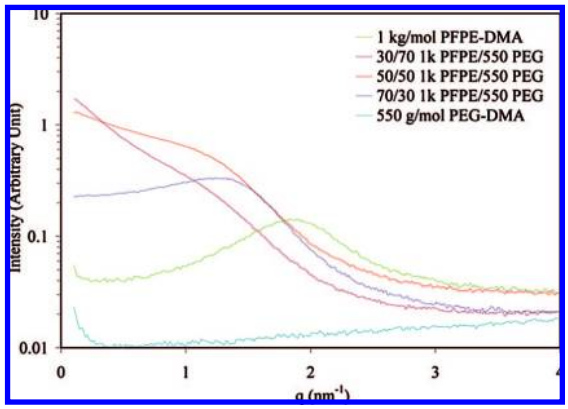

Figure 5. 1D SAXS data for optically transparent films of cross-linked 1k PFPE/550 PEG blends at various composition ratios. Also shown are the corresponding cross-linked homopolymers. All the data were acquired on the same instrument over a 2-h time period and were not shifted on the *y*-axis.

observed with light PEG-enriched domains as large as 400 nm being separated by spongelike PFPE-enriched domains of 71.7 ± 21.1 nm. As more of the 1 kg/mol PFPE-DMA was incorporated into the PEG matrix, the cocontinuous biphasic system changed to a matrix fully composed of isolated polydisperse domains of 50−250 nm (Figure 4e) with some domains aggregated together to form larger domains. With domain sizes above several hundred nanometers, both 30/70 1k PFPE/550 PEG and 50/50 1k PFPE/550 PEG blends appeared to be hazy as shown in Figure 1. As the content of the 1 kg/mol PFPE-DMA was increased to 70%, the cross section appeared to be less heterogeneous with uniform domains of 61.3 ± 13.5 nm resulting in a clear film (Figure 4f).

Because of the domain size of the macrophase-separated blends being beyond the working range of AFM, optical microscopy was used to study the bulk morphology of the opaque 4k PFPE/PEG blends. As shown in Figure 6a, an ultrathin film of 30/70 4k PFPE/550 PEG blend was found to have spherical PFPE-enriched domains randomly distributed in a continuous PEG matrix with domain sizes of 1−90 μm. The polydisperse PFPE-enriched domains in this blend were seen to be isolated from each other. It was particularly interesting to find some smaller spheres of 1−5 μm enclosed inside the larger spherical domains. The phase separation behavior looks similar for the 50/50 4k PFPE/550 PEG blend as shown in Figure 6b; however, no spheres as large as 90 μm were seen. Most of the domains were 40−50 μm in diameter. As the content of the 4 kg/mol PFPE-DMA was increased to 70%, the size of the PFPE-enriched domains decreased dramatically to less than 10 μm with most of the spheres connected to each other in Figure 6c.

When the higher molar mass 750 g/mol PEG-DMA was used, the series of 4k PFPE/750 PEG blends appeared by optical microscopy to be more heterogeneous and phase separated. As seen in Figure 6d, for the 30/70 4k PFPE/750 PEG blend most of the spherical PFPE-enriched domains were less than 50 μm. The morphology dramatically changed though for the 50/50 4k PFPE/750 PEG blend as the cross section was mostly filled with large PFPE-enriched spheres of 40−100 μm while small spherical PFPE-enriched domains were rarely seen outside of these larger ones. Instead, almost all of the small PFPE-enriched domains were located inside the larger spheres. However, as the composition ratio was increased further to 70/30 4k PFPE/750 PEG, the morphology significantly changed again as the large PFPE-enriched domains disappeared and the small PFPE-enriched domains of 1−15 μm were dispersed in a PEG-enriched matrix. A less compatible system was generally found for 4k PFPE/750 PEG blends with both the size and number of spherical PFPE-enriched domains greater than the counterparts in the 4k PFPE/550 PEG blends.

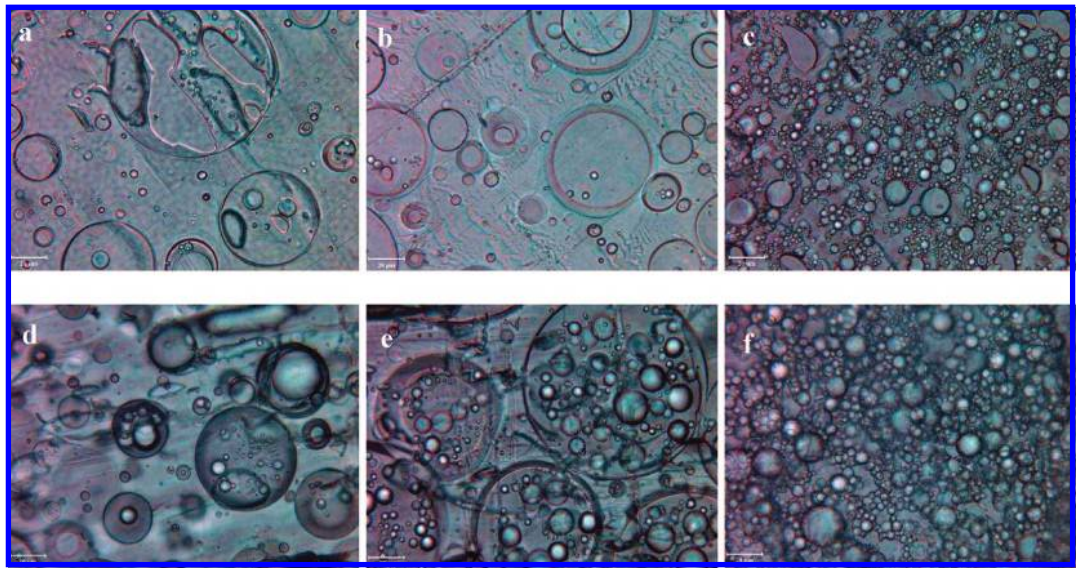

Figure 6. Morphology of cross sections of cured blends by optical microscopy. (a) 30/70 4k PFPE/550 PEG, (b) 50/50 4k PFPE/550 PEG, (c) 70/30 4k PFPE/550 PEG, (d) 30/70 4k PFPE/750 PEG, (e) 50/50 4k PFPE/750 PEG, and (f) 70/30 4k PFPE/750 PEG. The cross section thickness is 5 μm for 4k PFPE/550 PEG blends and 10 μm for 4k PFPE/750 PEG blends. The magnification is 40× with a scale bar of 20 μm.

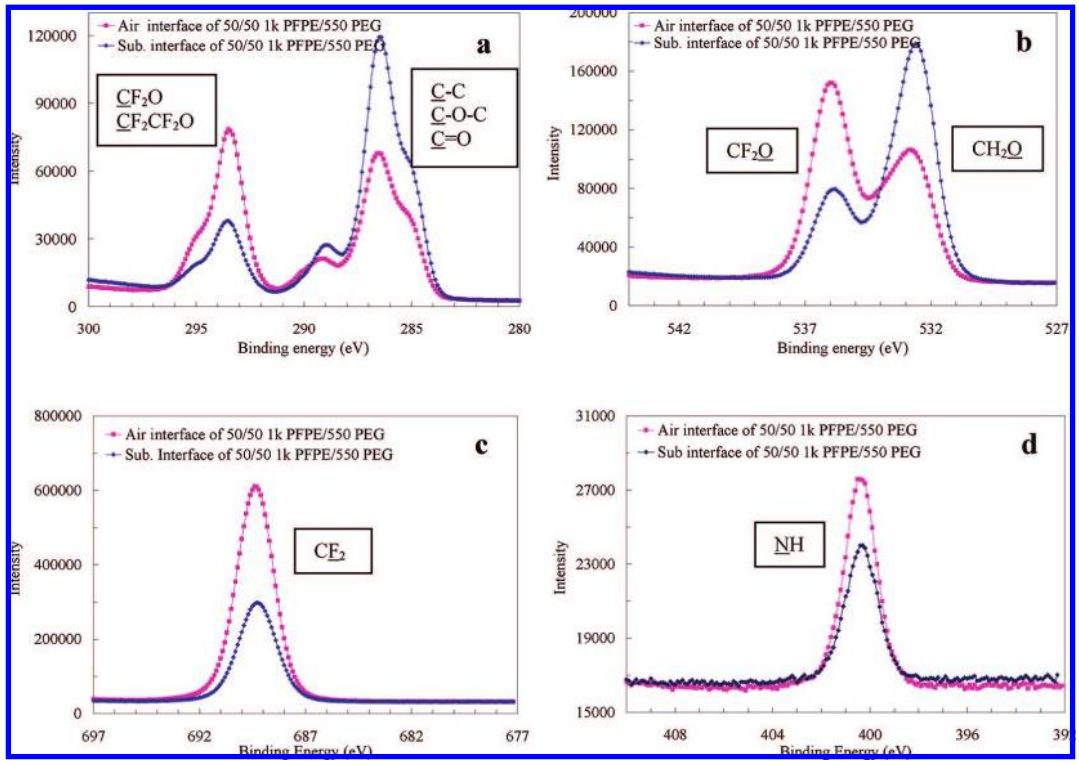

Figure 7. Representative XPS high-resolution spectra for both air and glass interfaces of cross-linked 50/50 1k PFPE/550 PEG. (a) C_{1s}, (b) O_{1s}, (c) F_{1s}, and (d) N_{1s}.

The mechanical properties of these amphiphilic films were analyzed using an Instron (Table 1). Young's modulus was calculated from the slope of the initial linear section (up to 2% of elongation) of the stress−strain curve. For 1k PFPE/PEG films, the moduli were increased by incorporating the more rigid 1 kg/mol PFPE-DMA into the blends. As the content of the 1 kg/mol PFPE-DMA was increased to 70%, the modulus increased to 70 MPa, almost double that of the 550 g/mol PEG-DMA (40 MPa). On the other hand, the moduli of the opaque 4k PFPE/PEG blends were much lower than those for 1k PFPE/PEG blends mainly because of much lower cross-link density. The characteristics of tunable mechanical strength and the unique fluorophilic/hydrophilic nature of these amphiphilic blends provide flexibility to design these materials for a variety of applications based on the specific requirements of the application.

PEG-based materials are well-known to nonspecifically resist protein adsorption.[26−28] However, most of the previously reported cross-linked PEG-based networks swell easily with high water uptake to form hydrogels. These swollen hydrogel networks are too brittle and weak to be used as antifouling coatings.[29]PFPEs are highly water resistant because of their

hydrophobic fluorinated structure. The hydrophobicity of PFPEs coupled with its bulk properties are expected to generate amphiphilic networks that would be mechanically robust with reduced swelling when PFPEs are incorporated into a PEG matrix. Herein, the water swelling ratio was carefully studied for all cured PFPE/PEG blends by evaluating the weight difference before and after being soaked in deionized water for 24, 48, and 72 h. No difference in transparency was observed for all samples after being soaked in water for 72 h. As shown in Table 1, the swelling ratios for the 1 and 4 kg/mol PFPE-DMAs were very low, even less than 1% after being soaked in water for 72 h, which is negligible compared with those for PEG homopolymers (27% for the 550 g/mol PEG-DMA and 51% for the 750 g/mol PEG-DMA). With its highly hydrophobic nature, swelling ratios for all blends of PFPE and PEG were decreased upon increasing the composition ratio of PFPE. For example, the optically transparent 1k PFPE/550 PEG blends, with a 30/70 composition weight ratio, swelled approximately 14 wt % for the composition ratio of 30/70. But as the content of the 1 kg/mol PFPE-DMA was increased to 50%, the sample swelled 7.5 wt %, and the swelling was further decreased to 2.5 wt % when the content of the 1 kg/mol PFPE-DMA in the blend was increased to 70%. It is believed that the water uptake can be reduced further by increasing the cross-link density of the PFPE. Additional studies showed that the swelling ratios of these blends remain unchanged in water for months. The high stability and durability of these robust materials would allow them to remain operational for an extended period in an underwater environment.

The surface properties of these amphiphilic blends were investigated as to what kind of interface would be achieved when hydrophilic PEG and hydrophobic PFPE are blended together to form uniform networks. High asymmetry was observed for these amphiphilic PFPE/PEG films in measuring the static contact angle on both the air and substrate interfaces. Generally, the air interface was found to be hydrophobic with a static contact angle of approximately 110°, while the substrate interface was hydrophilic with a static contact angle ranging from 57° to 75°, varying as a function of the composition ratio and molar mass (Table 1). Relatively high contact angles (>125°) on the air interfaces of the opaque 70/30 4k PFPE/550 PEG, 50/50 4k PFPE/750 PEG, and 70/30 4k PFPE/750 PEG films are believed to be caused by the high surface roughness due to macrophase separation on these interfaces. Slightly asymmetric surfaces have been previously reported on fluorinated surfaces, but to our knowledge, there have been no reports in the literature describing an amphiphilic blend with such highly asymmetric interfaces without any special chemical or physical treatments.[25,30,31] It is believed that the high asymmetry is introduced when the interfaces are formed under various polar environments.

The chemical compositions of the air and substrate interfaces of a cured 50/50 1k PFPE/550 PEG film were identified to reveal the surface asymmetry by XPS scans as summarized in Table 2. The overall chemical composition of the air interface of the blend film was very similar to the air interface of the cured 1 kg/mol PFPE-DMA homopolymer. The fluorine concentration was much higher on the air interface of the blend film compared to the substrate interface of the same film. High-resolution XPS spectroscopy was performed to further reveal the local chemical disparity on each interface of the 50/50 1k PFPE/550 PEG film. As seen in Figure 7a, while two main peaks with similar intensity were found in the C_{1s} spectrum of the air interface of the blend film, corresponding to the overlap of fluorocarbon peaks at CF_2O (~294.9 eV), CF_2CF_2O (~293.5 eV) and the overlap of hydrocarbon peaks at C═O (~288.9 eV), C−O−C (~286.4 eV), and C−C (~284.9 eV), the C_{1s} spectrum of the substrate interface exhibits much higher intensity for hydrocarbon peaks, indicative of an enriching of the polar PEG component. The data in the O_{1s} spectra in Figure 7b is very consistent with that in the C_{1s} spectra. The dominant peak in the O_{1s} spectra was attributed to CF_2O (~535.9 eV) on the air interface and to C−O (~532.5 eV) on the substrate interface. Both higher fluorine and nitrogen compositions were further discerned in the F_{1s} (689.2 eV) and N_{1s} (400.2 eV) spectra of the air interface of the blend film as shown in Figure 7c,d. All of these XPS results corroborate the results of the static contact angle measurements. For the cross-linked PFPE/PEG networks, the nonpolar PFPE chains gravitate to the less polar air interface to create a highly hydrophobic surface, while the hydrophilic polar PEG chains are attracted to the polar substrate interface, leading to its hydrophilic characteristic.

Table 2. Surface Chemical Mass Compositions of 50/50 1k PFPE/550 PEG Blend Identified by XPS Spectra

	C_{1s}	O_{1s}	F_{1s}	N_{1s}
air interface: blend	28.5	20.2	50.2	1.1
substrate interface: blend	40.8	26.2	32.0	1.0
air interface: 1 kg/mol PFPE-DMA	25.7	18.4	54.4	1.6

Protein Adsorption. Self-assembled oligo(ethylene glycol) monolayers are a well-established model for studying protein resistance behaviors.[26,27] There have been numerous reports on their nonspecific protein-resistant properties in the past two decades.[28] However, the disadvantage of this model is that the OEG SAMs are unstable and rapidly autoxidize, especially in the presence of oxygen and biochemically relevant transition-metal ions.[32−34] It was also reported that grafted PEG brushes gradually lose their protein repulsive properties above 35 °C.[35] The potential of our PFPE/PEG blends as alternative nonfouling coating materials was explored. Fibrinogen adsorption on optically transparent 1k PFPE/PEG thin films was determined by an ELISA method. A gold surface with equivalently banded OEG SAMs was set up as the negative control, and a bare glass substrate was set up as the positive control. The enzyme-induced color change in the protein solution was recorded at 450 nm as absorbance, which is proportional to the amount of antibody bound to surfaces. To better compare the amount of fibrinogen on each surface, the absorbance on the glass substrate was set

(26) Bain, C. D.; Whitesides, G. M. *Science* **1988**, *240*, 62.
(27) Prime, K. L.; Whitesides, G. M. *Science* **1991**, *252*, 1164.
(28) (a) Mrksich, M.; Sigal, G. B.; Whitesides, G. M. *Langmuir* **1995**, *11*, 4383. (b) Ostuni, E.; Chapman, R. G.; Holmlin, R. E.; Takayama, S.; Whitesides, G. M. *Langmuir* **2001**, *17*, 5605. (c) Prime, K. L.; Whitesides, G. M. *J. Am. Chem. Soc.* **1993**, *115*, 10714.
(29) Priola, A.; Gorrelino, G.; Ferrero, F.; Malucelli, G. *Polymer* **1993**, *34*, 3653.
(30) Yilgor, I.; Riffle, J. S.; Wilkes, G. L.; McGrath, J. E. *Polym. Bull.* **1982**, *8*, 535.
(31) Van Der Grinten, M. G. D.; Clough, A. S.; Shearmur, T. E.; Bongiovanni, R.; Priola, A. *J. Colloid Interface Sci.* **1996**, *182*, 511.
(32) Ostuni, E.; Chapman, R. G.; Holmlin, R. K.; Takayama, S.; Whitesides, G. M. *Langmuir* **2001**, *17*, 5605.
(33) Chen, S.; Zheng, J.; Li, L.; Jiang, S. *J. Am. Chem. Soc.* **2005**, *127*, 14473.
(34) Crouzet, C.; Decker, C.; Marchal, J. *Makromol. Chem.* **1976**, *177*, 145.
(35) Leckband, D.; Sheth, S.; Halperin, A.; Whitesides, G. M.; Laibinis, P. E. *J. Phys. Chem. B* **1998**, *10*, 1125.

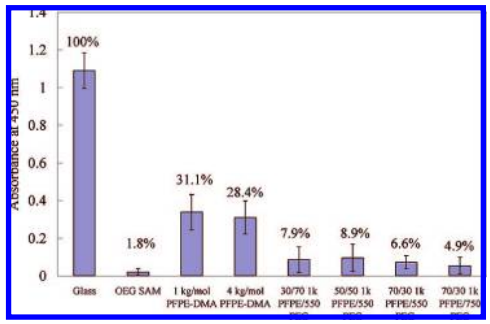

Figure 8. Amount of adsorbed fibrinogen from 1 mg/mL solution measured by ELISA. The data at the top of each of the columns is the relative adsorption values (mean ± SD %).

as 100% as relative adsorption. As shown in Figure 8, both PFPE surfaces demonstrated a certain level of resistance characteristic to fibrinogen with an average relative adsorption of approximately 30%, which was much higher than that on OEG SAMs (2%). However, the relative adsorption was significantly reduced by incorporating PEG into the PFPE networks. For example, the relative protein adsorption decreased from 31 to 7% in going from the 1 kg/mol PFPE-DMA surface to the 70/30 1k PFPE/550 PEG blend surface. Little difference on fibrinogen adsorption was found between the three 1k PFPE/550 PEG blend samples, which indicates that a high composition ratio of PEG in the PFPE network is not necessary to maintain the protein-resistant capability of these amphiphilic blends.

Conclusions

We studied the compatibility behaviors between fluorophilic PFPEs and hydrophilic PEGs. Clear liquid blends were achieved between the low molar mass 1 kg/mol PFPE-DMA and the 550 g/mol PEG-DMA in all composition ratios. The liquid blends of the 1 kg/mol PFPE-DMA with the higher molar mass 750 g/mol PEG-DMA turned from slightly hazy to clear with decreasing content of the 750 g/mol PEG-DMA. Optically opaque blends were obtained when the higher molar mass 4 kg/mol PFPE-DMA was mixed with either the 550 or 750 g/mol PEG-DMA. All of these liquid blends with dimethacryloxy functional end groups were easily cured free radically in one step to form optically transparent or opaque free-standing elastomeric films. The complex morphologies given by DMTA, DSC, and microscopy methods are consistent. It was indicated that nanophase separation occurs for the clear to hazy 1k PFPE/PEG blends while macrophase separation with domain sizes of 1−100 μm was generally observed for the opaque 4k PFPE/PEG blends. Compared with that of the cured PEG-DMA homopolymers, both mechanical strength and water resistance properties have been optimized by incorporating durable PFPE into a PEG matrix. Chemical compositions by XPS revealed the highly asymmetric interfaces with PFPE-enriched at the air interface and PEG-enriched at the substrate interface of the blends. Preliminary results show that the 1k PFPE/PEG amphiphilic surfaces were able to reduce the fibrinogen adsorption to a level comparable with that on an OEG SAM surface and a high incorporation of PEG into the blend is not necessary to keep a relatively low fibrinogen adsorption on the blend surfaces. With the combination of the high durability of PFPE and the nonfouling properties of PEG, the amphiphilic PFPE/PEG networks show good potential to be used as nonfouling coating materials.

Acknowledgment. This research was supported by the Office of Naval Research under Grant No. N00014-02-1-0185 as well as the STC program of the National Science Foundation for shared facilities. Parts of this work were carried out in the University of Minnesota I. T. Characterization Facility, which receives partial support from the NSF through the NNIN program. Sherryl Y. Yu-Su of UNC-CH was acknowledged for her individual help with the AFM along with Wallace Ambrose of the UNC-CH School of Dentistry for help preparing samples using a microtome. Dr. Carrie Donley of the UNC-CH performed the XPS experiments at the Chapel Hill Analytical & Nanofabrication Laboratory. We thank Prof. Lloyd M. Robeson for his invaluable help with T_g data analysis.

JA803991N